International Communications in Heat and Mass Transfer 110 (2020) 104397

Contents lists available at ScienceDirect

International Communications in Heat and Mass Transfer

journal homepage: www.elsevier.com/locate/ichmt

Experimental hydrothermal behavior of hybrid nanofluid for various particle ratios and comparison with other fluids in minichannel heat sink

Vivek Kumar, Jahar Sarkar*

Department of Mechanical Engineering, Indian Institute of Technology (B.H.U.), Varanasi, UP 221005, India

ARTICLE INFO

Keywords:
Minichannel heat sink
Hybrid nanofluid
Nanoparticle mixing ratio
Figure of merit
Performance index
Comparison

ABSTRACT

The effect of the particle mixture ratio in hybrid nanofluid on minichannel heat sink performance is analyzed experimentally. The heat sink, made of aluminium, contains nine parallel rectangular minichannels having cross section of 1 mm × 3 mm with 30 mm length. Total 0.01% volume concentration of Al_2O_3 and MWCNT nanoparticles for various mixing ratios (10:0, 8:2, 6:4, 4:6, 2:8 and 0:10) is used to synthesize water-based hybrid nanofluids. Different parameters as volumetric flow rate (0.17–0.5 LPM), fluid inlet temperature (20–40 °C) and heat flux (8.3 W/cm^2) are considered. Present Al_2O_3-MWCNT hybrid nanofluid is compared as well with hybrid nanofluids available in literature based on both thermophysical-transport and hydrothermal properties. Heat transfer coefficient, Nusselt number, pressure drop and friction factor increase with an increase in MWCNT fraction in hybrid nanofluid. Maximum heat transfer coefficient and pressure drop increments are 44.1% and 68.1%, respectively, for MWCNT nanofluid. Inlet fluid temperature has a negative effect on pressure drop and positive effect on heat transfer coefficient. Nusselt number to friction factor ratio is observed maximum at 6:4 mixing ratio of Al_2O_3 and MWCNT. Al_2O_3 + MWCNT (optimum mixing ratio of 6:4) hybrid nanofluid is found better as compared to existing hybrid nanofluids at total volume concentration of 0.01%.

1. Introduction

Over the past years, the issue faced by electronic devices for removing heat and ability improvement of the cooling system has achieved reasonable attention because of the miniaturization and rise of their heat flux generation [1]. Hence, to carry the components at their optimal operation, the thermal management of electronics devices is needed. The application of Mini/micro channel heat sink (MCHS) has been raised for decades due to materials preserving, space constraints, better heat transfer effectiveness, and lower coolant requirement than conventional heat exchangers [2,3]. Coolants of better thermophysical properties can be the good candidate to dissipate higher heat generated due to increasing demand for energy density. Hence, nanofluid or hybrid nanofluid (HyNf) has appeared as a feasible option due to their better heat transfer characteristics [4,5]. The hybrid nanofluids with perfect combination and proportion of nano-materials can be the best coolant to get superior hydrothermal characteristics and encouraged by their numerous heat transfer applications [5]. Alumina (Al_2O_3), a most common metal oxide nanoparticle, has been used by many researchers due to cheap, accessibility, chemical firmness and better heat transfer capability against pumping power [5]. As well as multi-walled carbon nanotube (MWCNT) is a viable candidate for nanofluids because of its remarkably high thermal conductivity and very high surface area [6]. Hence, to take advantages of Al_2O_3 and MWCNT, a combination of both can be the best option for hybrid nanofluid in MCHS.

Many experimental literatures are available on hydrothermal performance of mono particles suspended fluids in MCHS [7–10]. However, fewer literatures are available on MCHS using hybrid nanofluids. Selvakumar and Suresh [11] experimented thermo-hydraulic behavior of minichannel using hybrid nanofluids and found 24.35% and 12.61% augmentation in the convective heat transfer coefficient and pumping power, respectively. Ahammed et al. [12] experimented on the effect of graphene–alumina mixture based nanofluids for cooling application in minichannel and found a better enhancement of 63.13% in heat transfer coefficient. Nimmagadda and Venkatasubbaiah [13] did the experiment on microchannel using Al_2O_3 + Ag hybrid nanofluid and revealed that Nusselt number increases with nanoparticles fraction. Bahiraei et al. [14] did the exergy analysis of minichannel using HyNf suspended with coated CNT and Fe_3O_4 nanoparticles and revealed that the entropy generation is minimum for the lower Fe_3O_4 concentration. Ho et al. [15] experimented on MCHS with Al_2O_3 + MEPCM/water hybrid nanofluid and concluded that the Al_2O_3 nanofluid performs superior to the Al_2O_3 + MEPCM hybrid nanofluid at higher Reynolds number. They also revealed that the cooling effectiveness of the

* Corresponding author.
E-mail address: jsarkar.mec@itbhu.ac.in (J. Sarkar).

https://doi.org/10.1016/j.icheatmasstransfer.2019.104397

Available online 19 November 2019

Nomenclature

A	Effective heat transfer area (m^2)
c_p	Specific heat (J. kg^{-1}. K^{-1})
d_h	Hydraulic diameter (mm)
f	Friction factor
h	Heat transfer coefficient (W. m^{-2}. K^{-1})
h_{ch}	Channel height (mm)
k	Thermal conductivity (W. m^{-1}. K^{-1})
$\dot{V}$	Volume flow rate (LPM)
Nu	Nusselt number ($Nu = hd_h/k$)
Δp	Pressure drop (Pa)
Pr	Prandtl number ($Pr = \mu c_p/k$)
$\dot{Q}$	Heat transfer rate (W)
Re	Reynolds number ($Re = \rho u d_h/\mu$)
T	Temperature (°C)
u	Velocity (m. s^{-1})
vol	Volume
w_{ch}	Channel width (mm)
L_{ch}	Channel length (mm)
MCHS	Mini/micro channel heat sink
HyNf	Hybrid nanofluid
PI	Performance index ($=(h_{HyNf}/h_{bf})/(\Delta p_{HyNf}/\Delta p_{bf})^{1/3}$)
FOM	Figure of merit ($=[k_{HyNf}/k_{bf}]^{5/7}[\mu_{bf}/\mu_{HyNf}]^{1/7}[(\rho c_p)_{HyNf}/(\rho c_p)_{bf}]^{2/7}$)

Greek symbols

η_f	fin efficiency
μ	Dynamic viscosity (Pa. s)
φ	Volume concentration
ρ	Density (kg. m^{-3})

Subscripts

bf	base fluid
ch	channel
in	inlet
out	outlet
s	surface

working fluids depends significantly on their flow rates through the MCHS and found an optimum value below which hybrid suspension provided better performance compared to single particles-based fluid. Rehman et al. [16,17] did an experimental study on copper foam-PCM based heat sink for electronics cooling and found better heat sink base temperature reduction. Hussien et al. [18] did an experimental study of MWCNTs/GNPs hybrid nanofluids in microtubes and found 58% enhancement in heat transfer coefficient. Goodarzi et al. [19] numerically investigated the heat transfer behavior of various configurated microchannel heat sinks using graphene-Ag/water hybrid nanofluid and concluded that the hybrid nanofluid performs better than the base fluid. Uysal et al. [20] did a numerical investigation in rectangular minichannel using Diamond-Fe_3O_4/Water HyNf and observed that hybrid nanofluid is better compared to the mono particles nanofluids with respect to hydrothermal characteristics. Kumar and Sarkar [21] did numerical and experimental study on hydrothermal characteristics of Al_2O_3-TiO_2/DI water HyNf in minichannel and observed improvement as compared to water. A numerical investigation has been carried out by Ambreen et al. [22] in a micro pin fin heat sink using Al_2O_3-Cu hybrid nanofluid. They found 25.14% enhancement in Nusselt number for diamond fins with nanofluids. Shahsavar et al. [23] carried out a numerical investigation in concentric minitube using Fe_3O_4/CNT/water hybrid nanofluid and found that non-Newtonian hybrid nanofluid is better as compared to Newtonian hybrid nanofluid in terms of heat transfer coefficient and effectiveness.

The hydrothermal characteristics of hybrid nanofluids are influenced by nanoparticle mixture ratio but still the studies are limited on this important topic. Esfe et al. [24] measured the dynamic viscosity of Al2O3-MWCNT/5 W50 oil by varying particle ratio with total volume concentration of 0.05% to 1% and observed the maximum 24% increment in viscosity. Charab et al. [25] measured the thermal conductivity Al_2O_3-TiO_2 bi-particle nanofluid with various mixing ratios for total 1 vol% and observed the maximum thermal conductivity increment up to 35.3% for 2:3 ratio. Thermophysical properties of TiO_2-SiO_2 mixture HyNf were investigated experimentally by Hamid et al. [26] with various mixing ratio. Maximum enhancement up to 16% was observed for

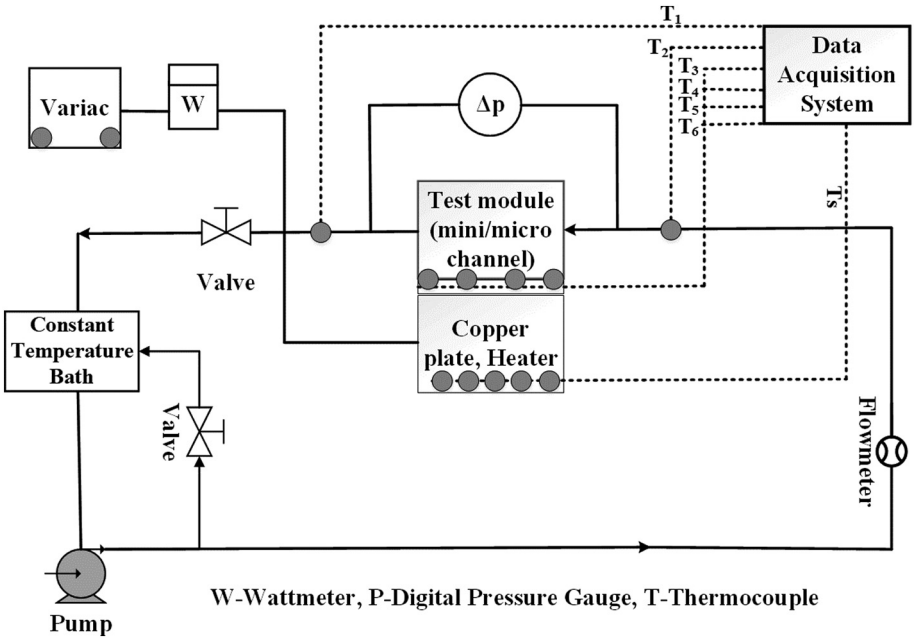

Fig. 1. Schematic diagram of minichannel heat sink test setup.

1:4 ratio and mixing ratio 5:5 for highest dynamic viscosity. They also studied the effect of mixing ratio on the cooling performance under turbulent flow considering TiO_2 and SiO_2 nanoparticles and found 1:4 and 2:3 mixing ratio of are favorable [27]. Moldoveanu et al. [28] measured the thermal conductivity of HyNf synthesized by Al_2O_3–SiO_2 in water and found that the HyNf having higher fraction of SiO_2 has higher thermal conductivity. The viscosity of Graphite-SiO_2 mixture-dispersed HyNf was experimentally investigated by Dalkılıç et al. [29] at different volume concentrations and found an increment of 36.12% in viscosity for 2% volume concentration. Siddiqui et al. [30] measured the thermophysical properties of HyNf by dispersing Cu-Al_2O_3 with various mixture ratios and achieved the superior thermal conductivity and good stability for the mixing ratio of 5:5. The thermophysical properties measurement of Al_2O_3–SiO_2/PAG nanolubricants was carried out by Zawawi et al. [31] for different particle mixture ratios and found the lowest property enhancement ratio for the particle ratio of 60:40. Kumar and Sarkar [21] observed hydrothermal performance of Al_2O_3-TiO_2/DI water HyNf in MCHS by changing mixing ratio and observed no optimum value. Thermophysical properties of MgO-TiO_2/water were investigated by Mousavi et al. [32] with different weight mixing ratios of MgO and TiO_2 nanoparticles. Thermal conductivity enhanced by 21.8% for mixing ratio of 80:20 equivalent to 0.3 vol% at 60 °C. Bhattad et al. [33] experimentally studied the hydrothermal characteristics of Al_2O_3-MWCNT/water hybrid nanofluids in plate heat exchanger by varying mixing ratio and found no optimum ratio.

Though, to the author best knowledge, none of the studies on minichannel heat sink considering dissimilar shaped nanoparticles combination is so far investigated. Furthermore, no performance comparison of various hybrid nanofluids was done for MCHS. Hence, experimentation on Al_2O_3-MWCNT (oxide-carbon nanotube mixture) HyNf with various mixture ratio in minichannel heat sink is conducted in the present study. Effects of volume flow rate, nanoparticle mixture ratio and inlet temperature on heat transfer coefficient, Nusselt number, pressure drop, friction factor, Nusselt number to friction factor ratio and performance index are discussed. Furthermore, the comparison of Al_2O_3-MWCNT hybrid nanofluid with hybrid nanofluids available in the literature based on thermophysical-transport as well as hydrothermal property is done to give an idea which one is better to design engineers.

2. Experimentation

2.1. Set-up description

The flow loop of the experimental facility is demonstrated in Fig. 1 and the details of the various components and loop of setup have been already reported [21]. Test section can be assembled and disassembled easily. Pressure transducer has been used to measure the pressure drop between header inlet and header outlet. A heater (having power of 50 W) located to the bottom of the heat sink. Constant and uniform heat flux magnitude of 8.3 W/cm^2 was supplied to the channel from the bottom side. Insulation is used for no heat losses from all other surfaces. NI data acquisition system (DAS) has been used to extract the data from the system. Photo image of minichannel heat sink along with schematic diagram is shown in Fig. 2.

The experiments were conducted using all the coolants at different inlet temperature (20–40 °C). Working fluids was supplied into the system from the reservoir using a pump. The heat flux is supplied when the flow rate reaches steady-state. Five K type thermocouples were inserted at different locations to the bottom of sink to measure average wall temperature. All the readings were measured using combination of computer and NI data acquisition system when system achieved steady-state condition, which was achieved in 40–50 min of the time interval. After data recording for a particular set, mass flow rate change to the next level and experiment were accomplished. Before test with another nanofluid, minichannels were cleaned by flowing water.

2.2. Hybrid nanofluid preparation and characterization

Al_2O_3–MWCNT/DI water hybrid nanofluid was synthesized by employing a two-step method in which particles are dispersed and mixed in the base fluid. Al_2O_3 nanoparticles (diameter: 45 nm) produced by Alfa Aesar, USA and multiwall carbon nanotubes (diameter: 20 nm, Length: 2 μm) manufactured by Otto Chemie Pvt. Ltd. were dispersed in the DI water. Acid-treated multiwall carbon nanotube (MWCNT) is used in this investigation to make it hydrophilic to DI water. Al_2O_3 nanoparticle and MWCNT have been taken in the different ratio as 10:0, 8:2, 6:4, 4:6, 2:8 and 0:10, respectively to prepare HyNf of 0.01 vol% concentration. First, an electronic weighing machine (model: ATX224, SHIMADZU, Japan) has been used to measure the calculated amounts of nanoparticles. Afterward, this amount of nanoparticles was mixed in base fluid (distilled water). Then, Ultrasonicator (Labman Scientific Instruments, India) was used to sonicate the colloidal solution for 6–8 h to synthesis well-dispersed nanofluid without surfactant. Morphology and particle size were inspected by high resolution scanning electron microscopy (HR-SEM: Nova Nano SEM 450, FEI, USA). HR-SEM image of Al_2O_3-MWCNT based HyNf of 6:4 mixing ratio is projected in Fig. 3. Which predicts an even distribution of nanoparticles and Al_2O_3 has an average particle size < 50 nm. In Fig. 4, Photography of Al_2O_3 + MWCNT/DI water HyNf are shown just after preparation and after the next 48 h. From these photo images, it can be inferred that nanoparticles were not settled down after 2 days, and experiments were performed using homogenized hybrid nanofluids.

From the SEM image (Fig. 3), it can be observed that particles are uniformly distributed and similar homogeneity of particles distribution also observed from the SEM images of the other samples. The pH values of different samples taken from various positions of the container have been measured and obtained in the range of 7.71 to 7.74, which are highly deviated from the isoelectric points. Hence it ensures the better homogeneity and stability of the hybrid nanofluids due to the large repulsion among the nanoparticles [34]. Similarly, the density and viscosity of synthesized nanofluids were measured for the same different samples at room temperature and no significant change (i.e., viscosity values are obtained in the range of 1.19 to 1.24 cP) was observed between them. Homogeneity of degree approximately 98% was

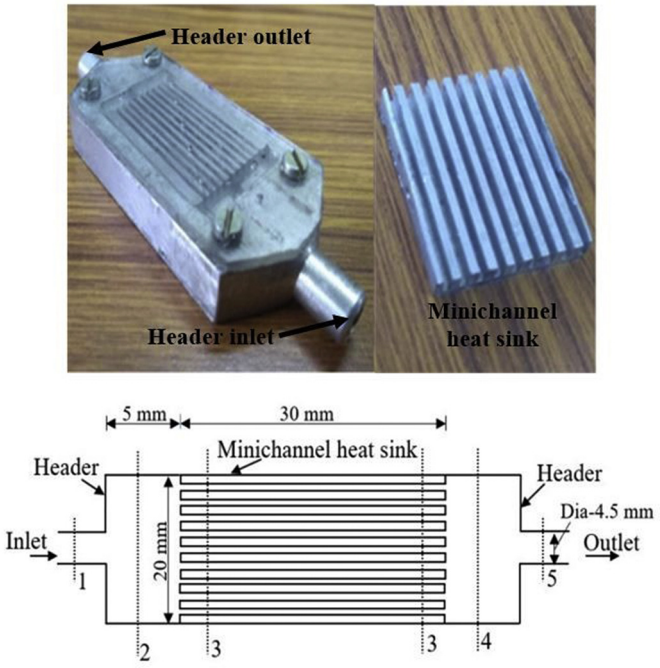

Fig. 2. Minichannel heat sink with schematic used in present experimental work.

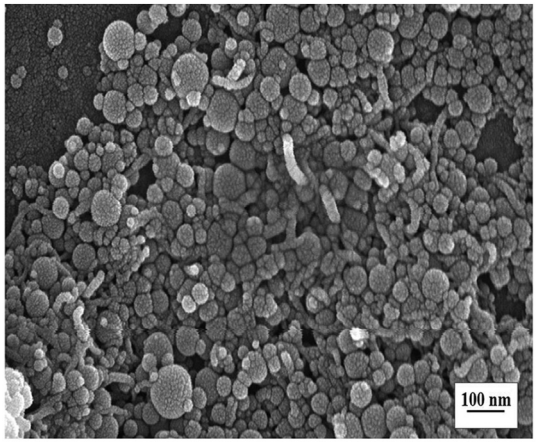

Fig. 3. SEM image of Al_2O_3-MWCNT hybrid nanofluid at 100 k magnification.

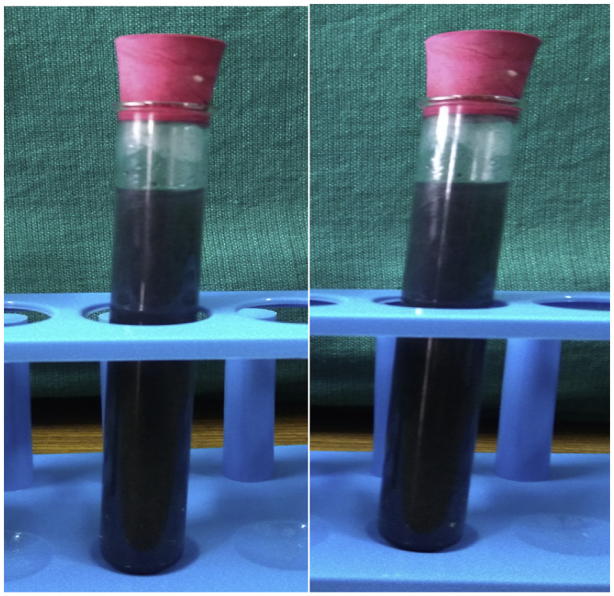

Fig. 4. Photography of Al_2O_3 + MWCNT/DI water hybrid nanofluid.

found for prepared HyNf depend on the experimentally measured properties. Above tests confirm the homogeneity of prepared hybrid nanofluids.

Thermophysical properties of HyNf have been experimentally measured using various measurement apparatuses. Information about apparatus has been given earlier elsewhere [21]. All the instruments were standardized before measuring data and measurement was repeated many times in order to get precise values.

2.3. Data reduction

The heat transfer rate was obtained by using volumetric flow rate, inlet and outlet temperatures measured from the experiment,

$$\dot{Q} = \dot{V}\rho c_p (T_{out} - T_{in}) \tag{1}$$

Then, the average convective heat transfer coefficient was evaluated by,

$$h = \frac{\dot{Q}}{A}\frac{\ln[(T_s - T_{in})/(T_s - T_{out})]}{[(T_s - T_{in}) - (T_s - T_{out})]} \tag{2}$$

Where, T_s is the average surface temperature (mean of five thermocouples reading, inserted at different locations to bottom of the heat sink) and A is the effective heat transfer area, calculated by,

$$A = N(w_{ch} + 2\eta_f h_{ch})L_{ch} \tag{3}$$

Where N is the number of channels, η_f is the fin efficiency, L_{ch}, w_{ch} and h_{ch} are the length, width and height of the channel, respectively.

Then, the Nusselt number (*Nu*) is given as,

$$Nu = \frac{hd_h}{k} \tag{4}$$

Where hydraulic diameter (d_h) of minichannel is given by,

$$d_h = \frac{2w_{ch}h_{ch}}{w_{ch} + h_{ch}} \tag{5}$$

Using flow rate, the Reynolds number (*Re*) was estimated by,

$$\mathrm{Re} = \frac{\rho \dot{V} d_h}{\mu N w_{ch} h_{ch}} \tag{6}$$

Using measured pressure drop (between inlet and exit ports), the pressure drop in the minichannel has been calculated by,

$$\Delta p = \Delta p_{\mathrm{Exp.}} - \rho g (Loss_{\mathrm{minor}}) \tag{7}$$

Where, $losses_{minor}$ = enlargement losses + contraction losses. Schematic of minichannel heat sink with headers is shown in Fig. 2. Schematic is divided into different sections (1–5). Based on enlargement and contraction losses in different sections [35], the total minor loss has been calculated by,

$$Loss_{\mathrm{minor}} = \frac{u_1^2}{2g}\left(1 - \left(\frac{A_1}{A_2}\right)\right)^2 + K_1\frac{u_3^2}{2g} + \frac{u_3^2}{2g}\left(1 - \left(\frac{N.A_3}{A_4}\right)\right)^2 + K_2\frac{u_5^2}{2g} \tag{8}$$

Where, $A_1 = A_5$, $A_2 = A_4$, $u_1 = \dot{V}/A_1$, $u_3 = \dot{V}/(NA_3)$, $A_3 = w_{ch}h_{ch}$ and $u_5 = \dot{V}/A_5$. K_1 depends upon A_3/A_2 ratio and K_2 depends upon A_5/A_4 ratio.

Then the friction factor has been calculated by,

$$f = \frac{2d_h\Delta p}{L_{ch}\rho u_3^2} \tag{9}$$

2.4. Uncertainty analysis

Using the uncertainties of measured variables (W_1, W_2, ……., W_n), the

uncertainties (W) of dependent variables (heat transfer coefficient, friction factor, etc)

have been estimated by Kline and McClintock [36] equation.

$$W = \left[\left(\frac{\partial R}{\partial X_1}W_1\right)^2 + \left(\frac{\partial R}{\partial X_2}W_2\right)^2 + \ldots\ldots\ldots\ldots\left(\frac{\partial R}{\partial X_n}W_n\right)^2\right]^{1/2} \tag{10}$$

Where, R is a function of independent variables (X_1, X_2……, X_n). The values of

uncertainty (W) obtained are given in Table 1.

3. Results and discussion

3.1. Validation

The validation for heat transfer aspect (Nusselt number) had been already presented in the authors' previous publication [21], which showed close prediction with existing correlations. The experimental data of friction factor obtained for Al_2O_3/DI water nanofluid is also compared with the existing correlation available in literature as shown in Fig. 5. It is observed that the experimental friction factor value while considering minor losses (enlargement losses and contraction losses) has good agreement with most of the existing correlations [37–40] for above *Re* = 200. For comparison with the available correlations, the

Table 1
The uncertainties during the experiments.

Variable	Uncertainty value (%)
Temperature	± 0.33
Volume flow rate	± 0.5
Pressure drop	± 0.25
Thermal conductivity	± 2.0
Viscosity	± 2.0
Density	± 2.0
Specific heat	± 2.0
Convective heat transfer coefficient	± 3.1
Friction factor	± 2.8
Nusselt number	± 3.8
Reynolds number	± 3.1

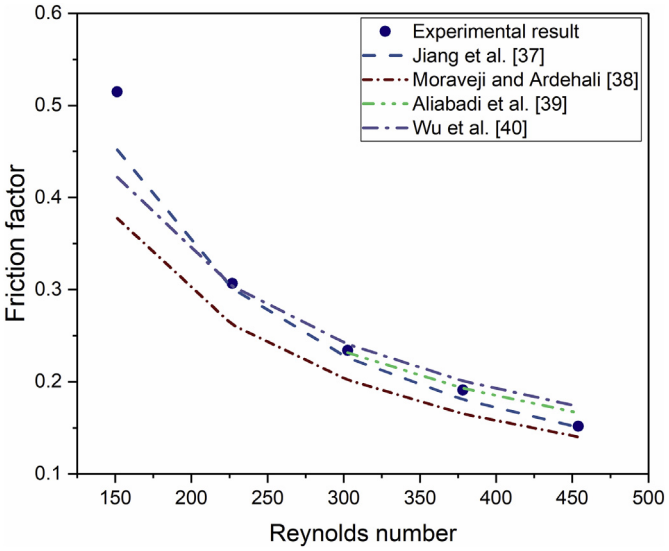

Fig. 5. Validation of friction factor with existing correlations.

friction factor was evaluated on the basis of the pressure drop in the minichannel only. In the present study, the pressure drop has been observed by pressure transducer between inlet and outlet of the header. Inlet and outlet headers are shown in Fig. 2. Thus, to calculate the pressure drop in minichannel, pressure losses in headers have been subtracted from the experimental data. Based on this calculated pressure drop, friction factor was obtained for validation. The experimental friction factor is best matching with the correlation developed by Jiang et al. [37].

3.2. Heat transfer characteristics

Variation of calculated heat transfer coefficient with the volume flow rate for studied hybrid nanofluids is depicted in Fig. 6 at the fluid inlet temperature of 30 °C. Different hybrid nanofluids were synthesized by changing the fraction of MWCNT and Al_2O_3 nanoparticles for a total volume concentration of 0.01%. Constant temperature bath having synchronized heating and cooling provisions before flowing into the channel is employed for maintaining constant inlet temperature. Heat transfer coefficient increases with the flow rate can be easily observed by the figures, which may be due to thinning of the thermal boundary layer. Enhancement in the heat transfer coefficient is observed with the addition of nanoparticles in the distilled water (base fluid), which is due to many reasons including thermal conductivity rise, various slip mechanisms and the effect of nano-fin and nano-porous. The heat carrier nanoparticles also contributed to these results along with the micro convection. As shown in figure, the heat transfer coefficient increases with increase in the proportion of MWCNT in the nanoparticle mixture. It is supported by the very high thermal conductivity of MWCNT nanoparticles. Another reason may be a higher specific surface area due to the higher aspect ratio of the carbon nanotube. This reason is supported by the fact that particles having large surface area accelerate heat dispersion in the fluid due to micro convection.

The effect of inlet temperature on heat transfer coefficient is shown in Fig. 7 at a volumetric flow rate of 0.33 LPM. Different inlet temperatures have been taken to claim the sustainability and flexibility of the current study for a wide range of atmospheric temperature globally. It exhibits from the figures that fluid inlet temperature has a positive effect on heat transfer coefficient. This may be attributed by the fact that the boundary layer becomes thinner due to decrease in viscosity with the increase in temperature. Heat transfer coefficient lifts with temperature for the same temperature difference because of the thinning of the thermal boundary layer. For MWCNT/DI water nanofluid, the heat transfer coefficient increases by 12.12% for the temperature increase from 20 °C to 40 °C. The heat transfer enhancement was considerably improved at higher working temperature because of the improvement of thermal properties. The increment of thermal conductivity of nanofluids is more meaningfully at higher operating temperature and hence temperature-dependent thermal conductivity may be another possible advantage for using the nanofluids as the high-temperature coolant. Maximum heat transfer coefficient is obtained for 0.01 vol% MWCNT/water nanofluid having the value of 4997.5 W/m^2K (44.02% higher as compared to base fluid).

For a specific heat sink, heat transfer due to conduction is constant because it depends on the material properties, heat sink dimensions and heat source. But heat transfer due to convection strongly depends upon the fluid and flow properties. Figs. 8–10 show the variation of Nusselt number with Reynolds number for different working fluids at the inlet temperatures of 20, 30 and 40 °C. It exhibits that Nusselt number increases as the Reynold number increases. The nanoparticle's dispersion in the base fluid augments the Nusselt number. The Nusselt number also shows dependency on the mixing ratio. Nusselt number shows the same trends similar to the heat transfer coefficient. As the MWCNT fraction increases in the HyNf, Nusselt number increases. The calculated Nusselt number has a maximum value of about 11.9 at 40 °C for MWCNT/DI water nanofluid. The maximum increment of 41.04% is found for MWCNT/DI water nanofluid over to DI water at Re = 446.9. As the Reynolds number is proportional to inlet velocity, the higher Reynold number means higher velocity. Movement and inter-collision of nanoparticles are increased with inlet velocity (Reynolds number), which enhances the heat transfer rate and hence enhancement of Nusselt Number. Improvement in Nusselt number was found when the

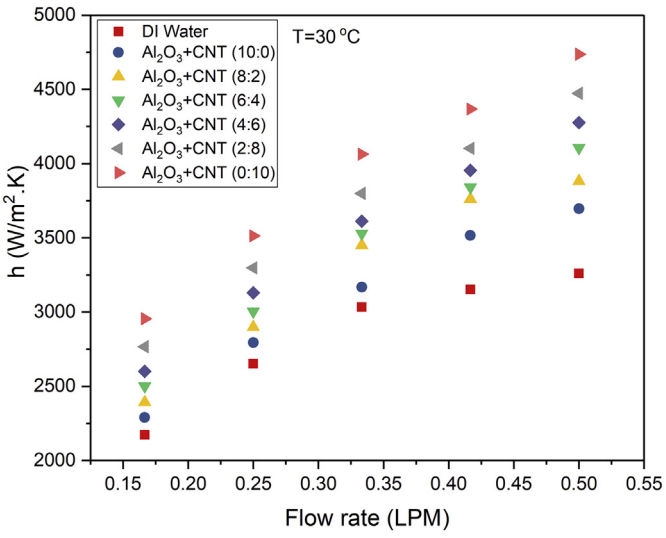

Fig. 6. Variation of heat transfer coefficient with flow rate (T_{in} = 30 °C).

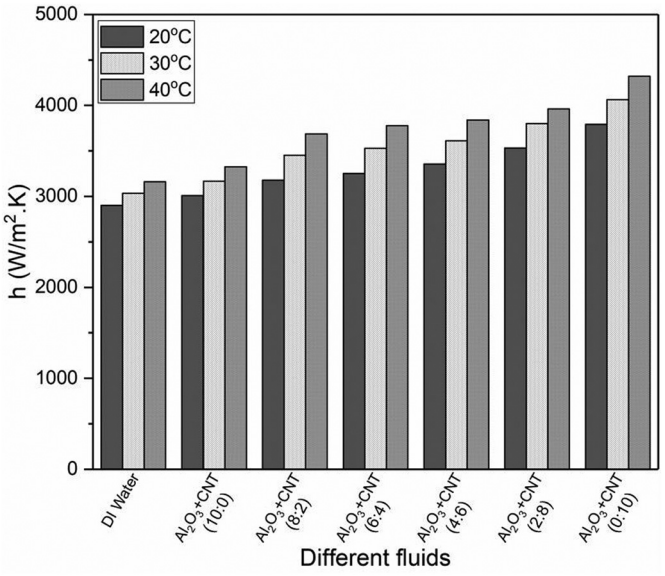

Fig. 7. Effect of inlet temperature on heat transfer coefficient at 0.33LPM.

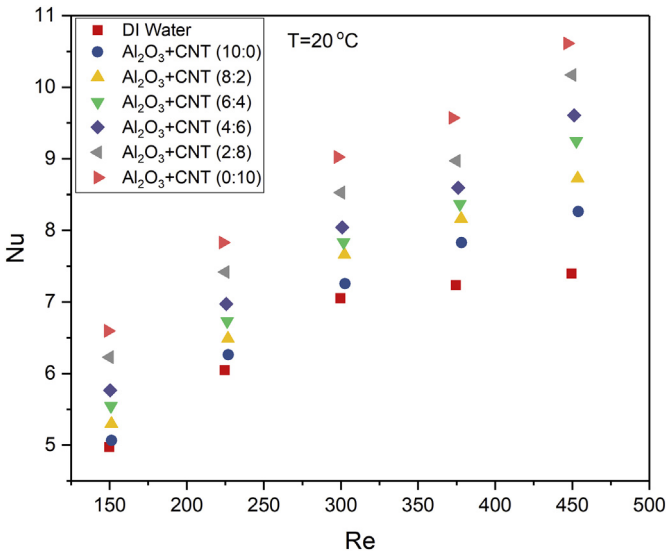

Fig. 8. Nusselt number vs Reynolds number for different working fluids (T_{in} = 20 °C).

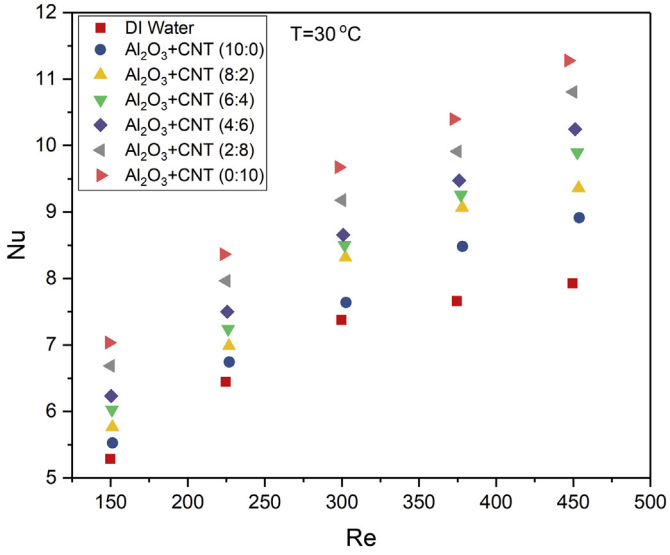

Fig. 9. Nusselt number vs Reynolds number for different working fluids (T_{in} = 30 °C).

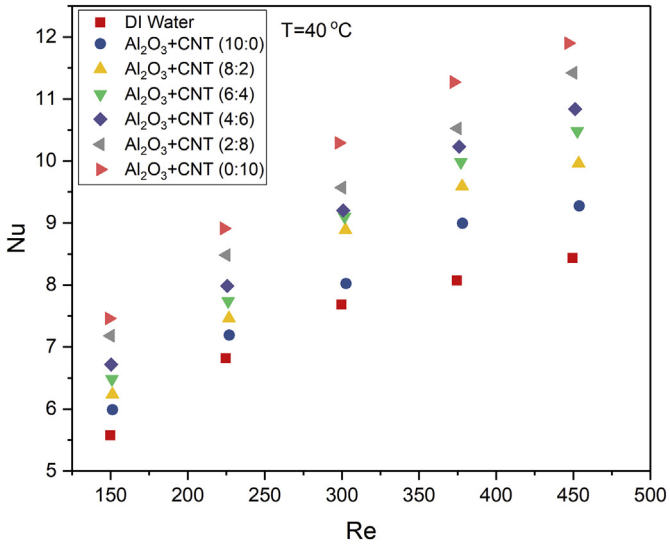

Fig. 10. Nusselt number vs Reynolds number for different working fluids (T_{in} = 40 °C).

temperature of inlet working fluid increases from 20 °C to 40 °C. The Nusselt number has been increased in the range of 12.3%–14.9% for all the coolants when inlet temperature increased from 20 °C to 40 °C.

3.3. Pressure drop characteristics

By adding the nanoparticles in the base fluid, improvement in the heat transfer performance is occurred but on the penalty of increment in pressure drop. The penalty in pressure drop by adding nanoparticles in different mixing ratio with flow rate is depicted in Fig. 11 at 30 °C inlet temperature. Generally, the density and viscosity are responsible for the pressure drop increment by adding nanoparticles. The flow rate (inlet velocity) is also accountable for increment in pressure drop. As the MWCNT fraction in the HyNf increases, the pressure drop increases with a faster rate. Maximum pressure drop is found 340.8 N/m^2 at 0.5LPM and 20 °C for MWCNT dispersed working fluid. The enhancement of 68.1% is observed for MWCNT/DI water nanofluid when compared to distilled water. Such enhancement in pressure drop for MWCNT/DI water may be due to its high surface area. Variation in pressure drop for different inlet temperature is shown in Fig. 12 at the volume flow rate of 0.33 LPM. Fluid inlet temperature shows a negative impact on pressure drop because viscosity decreases with temperature. As the temperature increases from 20 °C to 40 °C, decrement in the range of 10.2%–17.4% has been observed in pressure drop for all the working fluids. It is a well-known fact that pressure drop rises with volume flow rate (Reynold number) for the same cross-section, but it is revealed from Fig. 11 that the trend diverges at higher volume flow rate. It is attributed by the fact that pressure drop directly proportional to mass flux and viscosity, and mass flux has dominance over viscosity at high volume flow rate.

Figs. 13–15 illustrate the changing of friction factor as a function of *Re* for various working fluids in the range of inlet temperatures of 20–40 °C. It is predicted that a decrement in the friction factor is observed with *Re* due to dual effects of boundary layer thinning and mass velocity increase. With the addition of nanoparticles in the base fluid, the friction factor shows uplift trend due to the rise in viscosity and slip mechanism. Friction factor increases for the hybrid nanofluids over base fluid. It has a higher value as the concentration of MWCNT

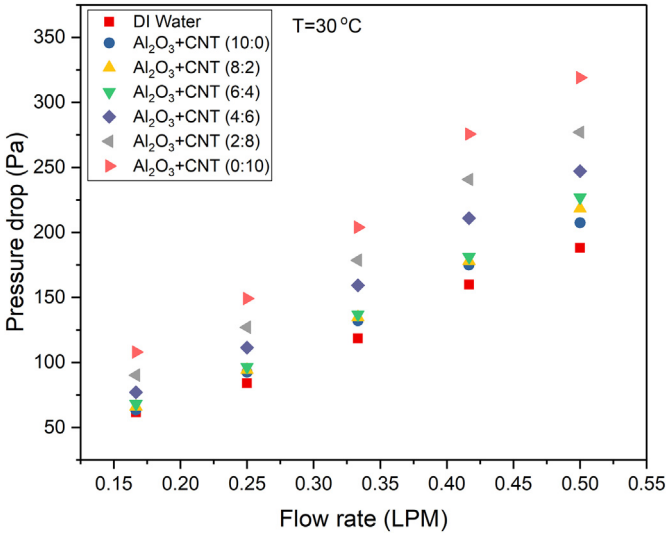

Fig. 11. Variation of pressure drop with flow rate (T_{in} = 30 °C).

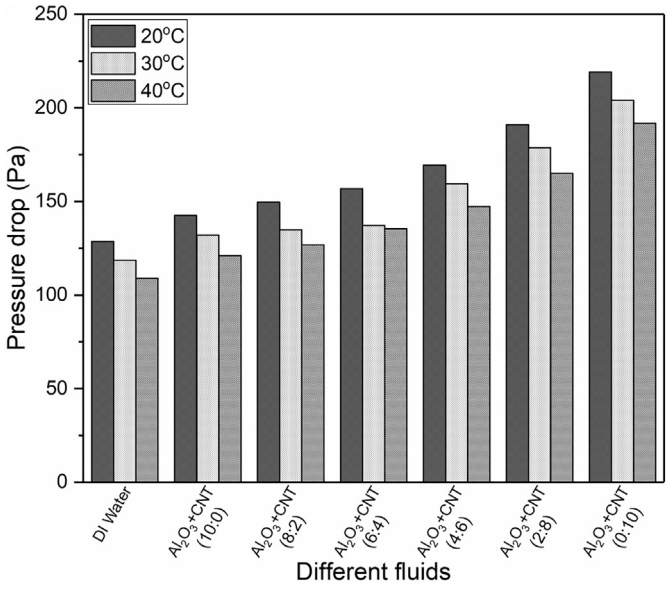

Fig. 12. Effect of inlet temperature on pressure drop at 0.33LPM for different coolants.

increases in the HyNf due to its high viscosity. At Re = 149, the maximum value of the friction factor for MWCNT/DI water nanofluid is approximate 1.05 at 20 °C. It is observed from the figures that the deviation of friction factor for different working fluids is significant at lower Reynolds number. This may be attributed by the fact that the viscosity is predominant at lower Reynolds number and it increases with increase in MWCNT concentration due to particle surface area and inter-particle attraction. Another reason may be rupturing of the boundary layer is predominant for MWCNT as compared to Al_2O_3 nanoparticles. Inlet temperature has an adverse effect on the friction factor for the same Reynolds number due to decrease in viscosity.

As predicted, with the changing of nanoparticles mixing ratio in hybrid nanofluid having the same total concentration, a notable change in friction factor is observed. Hence, it can be concluded that the hybrid nanofluid containing the mixing of nanoparticles with dissimilar morphology will exhibit different hydrodynamic characteristics.

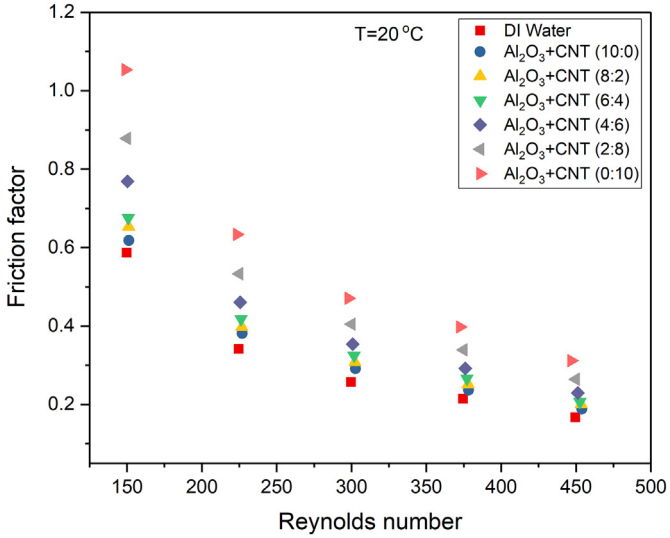

Fig. 13. Changing of Friction factor with Reynolds number (T_{in} = 20 °C).

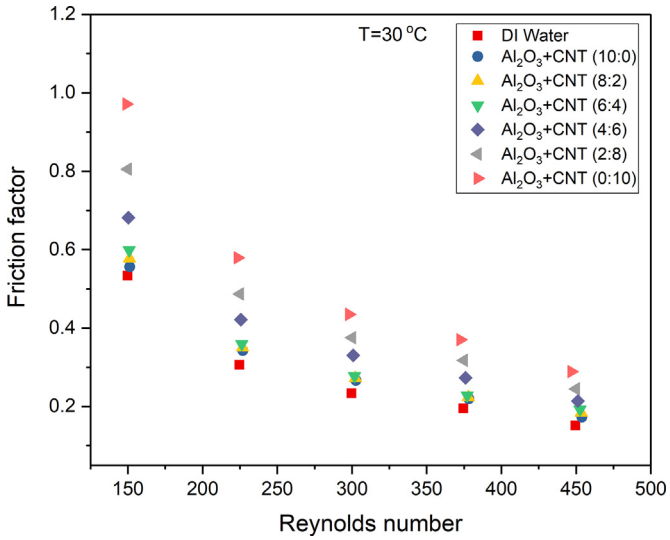

Fig. 14. Changing of Friction factor with Reynolds number (T_{in} = 30 °C).

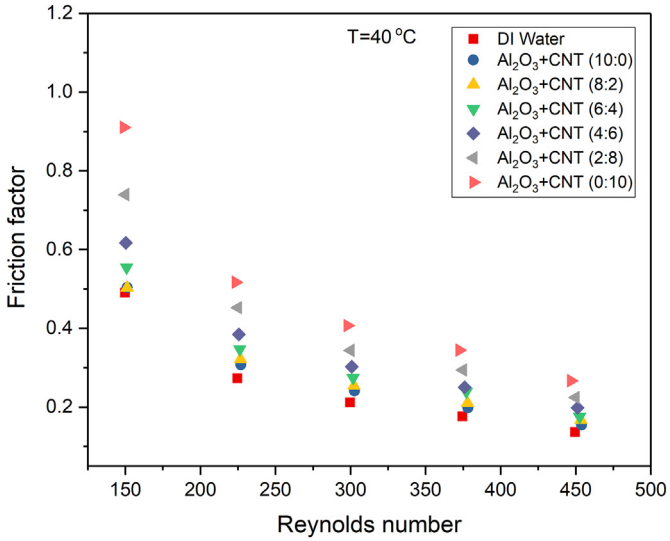

Fig. 15. Changing of Friction factor with Reynolds number (T_{in} = 40 °C).

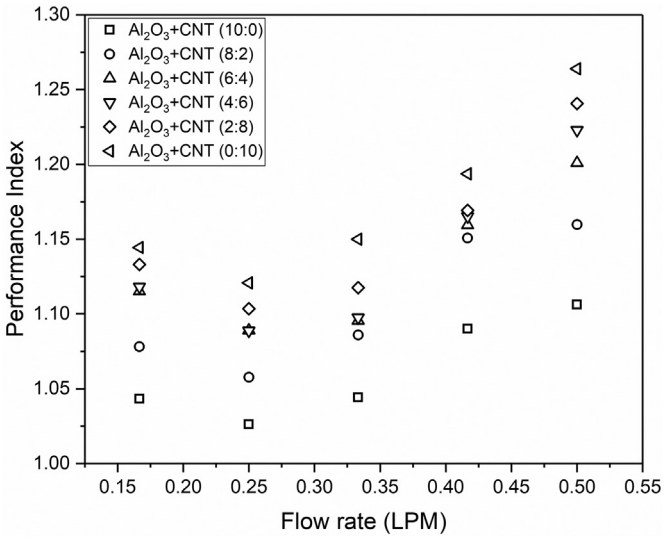

Fig. 16. Performance index vs flow rate for different working fluids.

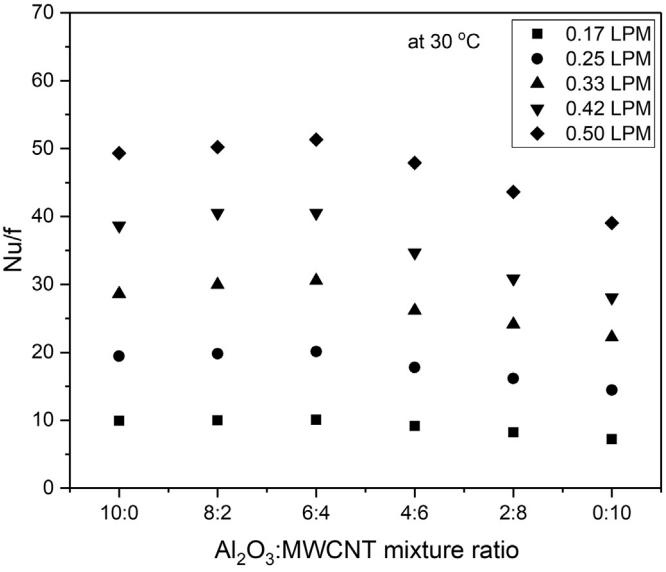

Fig. 17. Relative effect of mixture ratio on Nusselt number and friction factor (*Nu*/f).

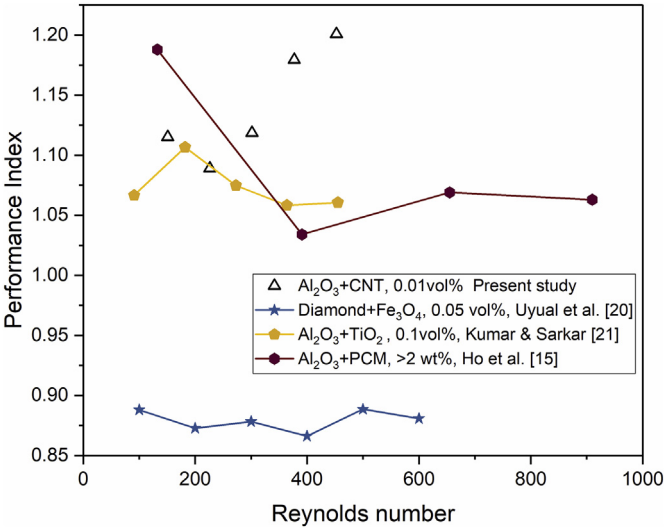

Fig. 18. Performance comparison of different hybrid nanofluids in micro-chennel heat sink.

3.4. Combined thermal-hydraulic characteristics

Heat transfer enhancement has been found with the addition of nanoparticles in the base fluid, as well as pressure drop might increases. So, heat transfer and pressure drop results do not deliver the correct conclusion, individually. Hence to accomplish the usefulness of hybrid nanofluid rather than conventional fluid, a comprehensive assessment factor i.e. performance index (PI) is introduced to find out the thermal performance of the system using hybrid nanofluids. The performance index is defined as,

$$PI = \left(\frac{h_{HyNf}}{h_{bf}}\right) / \left(\frac{\Delta p_{HyNf}}{\Delta p_{bf}}\right)^{1/3} \tag{11}$$

If PI > 1, the thermal performance of minichannel is increased and decreased for PI < 1. Fig. 16 shows the performance index of hybrid nanofluids at the inlet temperature of 30°C for different flow rates. For all the working fluids, performance index (PI) is above 1. Thus, it can be concluded that hybrid nanofluids are the better option as compared to distilled water in minichannel heat sink. It can be justifying that enhancement in pressure drop is less remarkable as compared to improvement in heat transfer coefficient. All the working fluids show the same trends, but performance index value increases as the MWCNT concentration increases. Performance index value first decreases with

Table 2
Property-based figure of merit (FOM) of different water-based hybrid nanofluids.

Authors	Temperature (°C)	Total particle concentration	Hybrid nanofluids	Thermal conductivity ratio (k_{HyNf}/k_{bf})	Dynamics viscosity ratio (μ_{HyNf}/μ_{bf})	FOM
Present study	30	0.01 vol%	Al_2O_3 + CNT (6:4)	1.0147	1.0439	1.0043
Siddiqui et al. [30]	–	0.01 vol%	Cu + Al_2O_3 (50:50) vol%	1.007	1.02	1.0021
Esfe et al. [24]	–	0.01 vol%	Ag + MgO (50:50) vol%	1.0272	1.1258	1.0022
Devarajan et al. [42]	40	0.05 vol%	CNT + Al_2O_3 (50:50) wt%	1.6374	1.948	1.2929
Sundar et al. [43]	30	0.05 vol%	ND-Fe_3O_4	1.035	1.2907	0.9881
Sundar et al. [44]	30	0.05 vol%	GO + Co_3O_4	1.026	1.085	1.0067
Sundar et al. [45]	30	0.1 vol%	CNT + Fe_3O_4 (26:74) wt %	1.133	1.1585	1.0705
Suresh et al. [46]	30	0.1 vol%	Al_2O_3 + Cu (9:1) wt%	1.01457	1.0237	1.0070
Mousavi et al. [32]	30	0.1 vol%	MgO + TiO_2 (50:50) wt%	1.0688	1.0599	1.0399
Bhattad et al. [47]	35	0.1 vol%	Al_2O_3 + SiC (4:1) vol%	1.0165	1.002986	1.0113
			Al_2O_3 + AlN (4:1) vol%	1.0147	1.00413	1.0098
			Al_2O_3 + MgO (4:1) vol%	1.009	1.00528	1.0056
			Al_2O_3 + CuO (4:1) vol%	1.00419	1.00987	1.0015
			Al_2O_3 + CNT (4:1) vol%	1.02448	1.01148	1.0157

the flow rate and then increases after a particular flow rate for all the nanofluids.

Variation of Nusselt number to friction factor ratio (*Nu/f*) with Al_2O_3 + MWCNT mixture ratio is shown in Fig. 17 for different flow rates. As the flow rate increases, Nu/f increases due to the predominance of Nu increase. As the MWCNT concentration increases in the HyNf, initially Nu/f increases and after a certain mixture ratio (optimum ratio) yielding maximum value, it starts decreasing. From Fig. 17, it is observed that 6:4 ratio is the optimum mixture ratio for the Al_2O_3-MWCNT (oxide-carbon nanotube) nanoparticle combination in minichannel heat sink. It is due to the dual effect of increasing Nussult number as well as friction factor with the increase in MWCNT proportion in Al_2O_3-MWCNT hybrid nanofluid.

3.5. Comparison with available fluids

The figure of merit (FOM) based on the properties in the laminar flow regime is described as Eq. 17 [41]. Here assumption has been made that volumetric specific heat is about to equal 1 based on the low concentration of nanoparticles mentioned by previous researchers [41]. Table 2 shows the properties-based figure of merit (FOM) of different water-based hybrid nanofluids. The results show that at 0.01 vol%, Al_2O_3 + CNT (6:4) hybrid nanofluid used in present study has highest FOM of 1.0043. Based on this result, we can conclude that Al_2O_3 + CNT based hybrid nanofluid is better as compared to other available nanofluids in literature at 0.01% volume concentration.

$$FOM = \left(\frac{k_{HyNf}}{k_{bf}}\right)^{5/7}\left(\frac{\mu_{bf}}{\mu_{HyNf}}\right)^{1/7}\left(\frac{(\rho c_p)_{HyNf}}{(\rho c_p)_{bf}}\right)^{2/7} \quad (12)$$

Fig. 18 depicts the comparison of the performance index of hybrid nanofluids used in the present study with the available fluids in existing literature for similar experimental conditions (similar channel aspect ratio and total particle volume concentration). It is observed that the Al_2O_3 + CNT hybrid nanofluid used in this study has comparatively better performance index as compared to Al_2O_3 + TiO_2, Al_2O_3 + PCM and Fe_3O_4 + Dimond hybrid nanofluid in minichannel heat sink. The maximum performance index value is approximately 1.20 for Al_2O_3 + CNT (6:4) hybrid nanofluid at Re = 452. The reason for such performance enhancement with Al_2O_3 + CNT hybrid nanofluid may be due to the higher surface area to volume ratio of CNT particles.

Thus, it may be concluded from Table 2 and Fig. 18 that the hybrid nanofluid, which shows the maximum Nusselt number to friction factor ratio (i.e. Al_2O_3 + CNT at 6:4 mixing ratio) is the better hybrid nanofluid composition as compared to others available nanofluids at volume concentration of 0.01%. Dissimilar to Al_3O_3 + TiO_2 [21], Al_2O_3 + CNT combination yields some optimum mixture ratio to get maximum hydrothermal performance in minichannel heat sink.

4. Concluding remarks

In the present paper, the effects of flow rate, inlet temperature and mixture ratio have been analyzed on minichannel using hybrid nanofluids. The hydrothermal characteristics of Al_2O_3-MWCNT hybrid nanofluid in minichannel are examined for dissimilar nanoparticles with mixing ratio (10:0 to 0:10) in total volume concentration of 0.01 vol%. Present hybrid nanofluid has been compared with existing hybrid nanofluids available in literature. Different conditions as range of flow rate (0.17–0.5 LPM), Reynolds number (100–500), different inlet temperature (20–40 °C) and heat flux 8.3 W/cm^2 was considered. Based on the investigation, the inferences are followed:

- ➢ Increase in flow rate, the fraction of MWCNT dispersed in base fluid and fluid inlet temperature has positive impact on convective heat transfer coefficient and Nusselt number. Nusselt number increases in the range of 12.3%–14.9% with the inlet temperature increase from 20 °C to 40 °C. *maximum* 44.02% enhancement of heat transfer coefficient was observed for MWCNT (10:0) hybrid nanofluid.
- ➢ With the increase in MWCNT concentration in the particle mixture of HyNf, the pressure drop and friction factor increase. A rise in pressure drop of 68.1% was observed for MWCNT nanofluid as compared to distilled water. Pressure drop reduces with inlet temperature. Reynolds number has an adverse effect on the friction factor.
- ➢ MWCNT/DI water nanofluid is more effective over Al_2O_3/DI water nanofluid in term of heat transfer coefficient.
- ➢ Hybrid nanofluids are better option as compared to distilled water in minichannel heat sink because all the hybrid nanofluids have performance index (PI) above 1.
- ➢ For hybrid nanofluid with dissimilar nanoparticle concentration, mixture ratio has a significant effect on heat transfer and pressure drop characteristics.
- ➢ The mixture ratio of 6:4 for Al_2O_3-MWCNT hybrid nanofluids is the optimum mixture ratio when considering hydrothermal characteristics in a minichannel heat sink.
- ➢ Al_2O_3 + MWCNT hybrid nanofluid at 6:4 mixing ratio is the better as compared to other available hybrid nanofluids at volume concentration of 0.01% in terms of both properties and hydrothermal characteristics.

References

[1] S. Ndao, Y. Peles, M.K. Jensen, Multi-objective thermal design optimization and comparative analysis of electronics cooling technologies, Int. J. Heat Mass Transf. 52 (2009) 4317–4326.

[2] I.A. Ghani, N.A.C. Sidik, N. Kamaruzaman, Hydrothermal performance of microchannel heat sink: the effect of channel design, Int. J. Heat Mass Transf. 107 (2017) 21–44.

[3] A. Dewan, P. Mahanta, K. Sumithra Raju, P. Suresh Kumar, Review of passive heat transfer augmentation techniques, Proc. Inst. Mech. Eng. Part A 218 (7) (2004) 509–527.

[4] G.M. Whitesides, The origins and the future of microfluidics, Nature 442 (2006) 368–373.

[5] H. Babar, H.M. Ali, Towards hybrid nanofluids: preparation, thermophysical properties, applications, and challenges, J. Mol. Liq. 281 (2019) 598–633.

[6] Z. Nikkhah, A. Karimipour, M.R. Safaei, P.F. Tehrani, M. Goodarzib, M. Dahari, S. Wongwises, Forced convective heat transfer of water/functionalized multi-walled carbon nanotube nanofluids in a microchannel with oscillating heat flux and slip boundary condition, Int. Commun. Heat Mass Tran. 68 (2015) 69–77.

[7] J. Zhang, Y. Diao, Y. Zhao, Y. Zhang, Thermal-hydraulic performance of SiC-water and Al_2O_3-water nanofluids in the minichannel, J. Heat Transf. 138 (2016) 021705.

[8] L. Nakharintr, P. Naphon, S. Wiriyasart, Effect of jet-plate spacing to jet diameter ratios on nanofluids heat transfer in a mini-channel heat sink, Int. J. Heat Mass Transf. 116 (2018) 352–361.

[9] C.J. Ho, J.C. Liao, C.H. Li, W.M. Yan, Mohammad Amani experimental study of cooling performance of water-based alumina nanofluid in a minichannel heat sink with MEPCM layer embedded in its ceiling, Int. Commun. Heat Mass Tran. 103 (2019) 1–6.

[10] A. Alfaryjat, L. Miron, H. Pop, V. Apostol, M.F. Stefanescu, A. Dobrovicescu, Experimental investigation of thermal and pressure performance in computer cooling systems using different types of nanofluids, Nanomaterials 9 (2019) 1231.

[11] P. Selvakumar, S. Suresh, Use of Al_2O_3–Cu/water hybrid nanofluid in an electronic heat sink, IEEE Trans. Compon. Packag. Manuf. Technol. 2 (2012) 1600–1607.

[12] N. Ahammed, L.G. Asirvatham, S. Wongwises, Entropy generation analysis of graphene–alumina hybrid nanofluid in multiport minichannel heat exchanger coupled with thermoelectric cooler, Int. J. Heat Mass Transf. 103 (2016) 1084–1097.

[13] R. Nimmagadda, K. Venkatasubbaiah, Experimental and multiphase analysis of nanofluids on the conjugate performance of micro-channel at low Reynolds numbers, Heat Mass Transf. 53 (2017) 2099–2115.

[14] M. Bahiraei, M. Berahmand, A. Shahsavar, Irreversibility analysis for flow of a non-Newtonian hybrid nanofluid containing coated CNT/Fe_3O_4 nanoparticles in a minichannel heat exchanger, Appl. Therm. Eng. 125 (2017) 1083–1093.

[15] C.J. Ho, W.C. Chen, W.M. Yan, P. Amani, Contribution of hybrid Al_2O_3-water nanofluid and PCM suspension to augment thermal performance of coolant in a minichannel heat sink, Int. J. Heat Mass Transf. 122 (2018) 651–659.

[16] T.U. Rehman, H.M. Ali, A. Saieed, W. Pao, M. Ali, Copper foam/PCMs based heat sinks: an experimental study for electronic cooling systems, Int. J. Heat Mass Transf. 127 (2018) 381–393.

[17] T.U. Rehman, H.M. Ali, Experimental investigation on paraffin wax integrated with copper foam based heat sinks for electronic components thermal cooling, Int. Commun. Heat Mass Tran. 98 (2018) 155–162.

[18] A.A. Hussien, M.Z.N.M. Yusop, W. Al-Kouz, E. Mahmoudi, M. Mehrali, Heat transfer and entropy generation abilities of MWCNTs/GNPs hybrid nanofluids in microtubes, Entropy 21 (480) (2019) 1–17.

[19] M. Goodarzi, I. Tlili, Z. Tian, M. Safaei, Efficiency assessment of using graphene nanoplatelets-silver/water nanofluids in microchannel heat sinks with different crosssections for electronics cooling, Int. J. Numer. Method H. (2019), https://doi.org/10.1108/HFF-12-2018-0730.
[20] C. Uysal, E. Gedik, A.J. Chamkha, A numerical analysis of laminar forced convection and entropy generation of a diamond-Fe_3O_4/water hybrid nanofluid in a rectangular minichannel, J. Appl. Fluid Mech. 12 (2019) 391–402.
[21] V. Kumar, J. Sarkar, Numerical and experimental investigations on heat transfer and pressure drop characteristics of Al_2O_3-TiO_2 hybrid nanofluid in minichannel heat sink with different mixture ratio, Powder Technol. 345 (2019) 717–727.
[22] T. Ambreen, A. Saleem, H.M. Ali, S.A. Shehzad, C.W. Park, Performance analysis of hybrid nanofluid in a heat sink equipped with sharp and streamlined micro pin-fins, Powder Technol. 355 (2019) 552–563.
[23] A. Shahsavar, A. Godini, P.T. Sardari, D. Toghraie, H. Salehipour, Impact of variable fluid properties on forced convection of Fe_3O_4/CNT/water hybrid nanofluid in a double-pipe mini-channel heat exchanger, J. Therm. Anal. Calorim. 137 (2019) 1031–1043.
[24] M.H. Esfe, A.A.A. Arani, M. Rezaie, W.M. Yan, A. Karimipour, Experimental determination of thermal conductivity and dynamic viscosity of Ag–MgO/water hybrid nanofluid, Int. Commun. Heat Mass Tran. 66 (2015) 189–195.
[25] A.A. Charab, S. Movahedirad, R. Norouzbeigi, Thermal conductivity of Al_2O_3 + TiO_2/water nanofluid: model development and experimental validation, Appl. Therm. Eng. 119 (2017) 42–51.
[26] K.A. Hamid, W.H. Azmi, M.F. Nabil, R. Mamat, K.V. Sharma, Experimental investigation of thermal conductivity and dynamic viscosity on nanoparticle mixture ratios of TiO_2-SiO_2 nanofluids, Int. J. Heat Mass Transf. 116 (2018) 1143–1152.
[27] K.A. Hamid, W.H. Azmi, M.F. Nabil, R. Mamat, Experimental investigation of nanoparticle mixture ratios on TiO_2-SiO_2 nanofluids heat transfer performance under turbulent flow, Int. J. Heat Mass Transf. 118 (2018) 617–627.
[28] G.M. Moldoveanu, G. Huminic, A.A. Minea, A. Huminic, Experimental study on thermal conductivity of stabilized Al_2O_3 and SiO_2 nanofluids and their hybrid, Int. J. Heat Mass Transf. 127 (2018) 450–457.
[29] A.S. Dalkılıç, Ö. Açıkgöz, B.O. Küçükyıldırım, A.A. Eker, B. Lüleci, C. Jumpholkul, S. Wongwises, Experimental investigation on the viscosity characteristics of water based SiO_2-graphite hybrid nanofluids, Int. Commun. Heat Mass Tran. 97 (2018) 30–38.
[30] F.R. Siddiqui, C.Y. Tso, K.C. Chan, S.C. Fu, C.Y.H. Chao, On trade-off for dispersion stability and thermal transport of Cu-Al_2O_3 hybrid nanofluid for various mixing ratios, Int. J. Heat Mass Transf. 132 (2019) 1200–1216.
[31] N.N.M. Zawawi, W.H. Azmi, M.Z. Sharif, G. Najafi, Experimental investigation on stability and thermo-physical properties of Al_2O_3–SiO_2/PAG nanolubricants with different nanoparticle ratios, J. Therm. Anal. Calorim. 135 (2019) 1243–1255.
[32] S.M. Mousavi, F. Esmaeilzadeh, X.P. Wang, A detailed investigation on the thermo-physical and rheological behaviour of MgO/TiO_2 aqueous dual hybrid nanofluid, J. Mol. Liq. 282 (2019) 323–339.
[33] A. Bhattad, J. Sarkar, P. Ghosh, Experimentation on effect of particle ratio on hydrothermal performance of plate heat exchanger using hybrid nanofluid, Appl. Therm. Eng. 162 (2019) 114309.
[34] H. Maddah, R. Aghayari, M. Mirzaee, M.H. Ahmadi, M. Sadeghzadeh, A.J. Chamkha, Factorial experimental design for the thermal performance of a double pipe heat exchanger using Al_2O_3-TiO_2 hybrid nanofluid, Int. Commun. Heat Mass Tran. 97 (2018) 92–102.
[35] Y.A. Cengal, J.M. Cimbala, Fluid Mechanics: Fundamentals and Applications, 1st ed., McGraw-Hill, New York, 2006, pp. 347–354.
[36] S.J. Kline, F.A. McClintock, Describing uncertainties in single-sample experiments, Mech. Eng. 75 (1953) 3–8.
[37] P.X. Jiang, M.H. Fan, G.S. Si, Z.P. Ren, Thermal–hydraulic performance of small-scale micro-channel and porous-media heat-exchangers, Int. J. Heat Mass Transf. 44 (2001) 1039–1051.
[38] M.K. Moraveji, R.M. Ardehali, CFD modeling (comparing single and two-phase approaches) on thermal performance of Al_2O_3/water nanofluid in mini-channel heat sink, Int. Commun. Heat Mass Tran. 44 (2013) 157–164.
[39] M.K. Aliabadi, S.E.H. Rad, F. Hormozi, Al_2O_3–water nanofluid inside wavy mini-channel with different cross-sections, J. Taiwan Inst. Chem. E. 58 (2016) 8–18.
[40] X. Wu, H. Wu, P. Cheng, Pressure drop and heat transfer of Al_2O_3-H_2O nanofluids through silicon microchannels, J. Micromech. Microeng. 19 (2009) 105020.
[41] S.H. Lee, H.J. Kim, S.P. Jang, Thermal performance criterion for nanofluids in laminar flow regime, J. Mech. Sci. Technol. 31 (2) (2017) 975–983.
[42] M. Devarajan, N.P. Krishnamurthy, M. Balasubramanian, B. Ramani, S. Wongwises, K.A. El-Naby, R. Sathyamurthy, Thermophysical properties of CNT and CNT/Al_2O_3 hybrid nanofluid, Micro Nano Lett. 13 (5) (2018) 617–621.
[43] L.S. Sundar, E.V. Ramana, M.P.F. Graça, M.K. Singh, A.C.M. Sousa, Nanodiamond-Fe_3O_4 nanofluids: preparation and measurement of viscosity, electrical and thermal conductivities, Int. Commun. Heat Mass Tran. 73 (2016) 62–74.
[44] L.S. Sundar, M.K. Singh, M.C. Ferro, A.C.M. Sousa, Experimental investigation of the thermal transport properties of graphene oxide/Co_3O_4 hybrid nanofluids, Int. Commun. Heat Mass Tran. 84 (2017) 1–10.
[45] L.S. Sundar, M.K. Singh, A.C.M. Sousa, Enhanced heat transfer and friction factor of MWCNT–Fe_3O_4/water hybrid nanofluids, Int. Commun. Heat Mass Tran. 52 (2014) 73–83.
[46] S. Suresh, K.P. Venkitaraj, P. Selvakumar, M. Chandrasekar, Synthesis of Al_2O_3–Cu/water hybrid nanofluids using two step method and its thermo physical properties, Colloids Surf. A 388 (2011) 41–48.
[47] A. Bhattad, J. Sarkar, P. Ghosh, Hydrothermal performance of different alumina hybrid nanofluid types in plate heat exchanger, J. Therm. Anal. Calorim. (2019), https://doi.org/10.1007/s10973-019-08682-y.